Characterisation of biological effects of a novel protein kinase D inhibitor in endothelial cells

Ian M Evans, Azadeh Bagherzadeh, Mark Charles, Tony Raynham, Chris Ireson, Alexandra Boakes, Lloyd Kelland, Ian C Zachary

CHARACTERISATION OF BIOLOGICAL EFFECTS OF A NOVEL PROTEIN KINASE D INHIBITOR IN ENDOTHELIAL CELLS

Ian M. Evans[1^], Azadeh Bagherzadeh[2], Mark Charles[2], Tony Raynham[2], Chris Ireson[2], Alexandra Boakes[2], Lloyd Kelland[2], and Ian C. Zachary[1^]

[1]Centre for Cardiovascular Biology and Medicine, Department of Medicine, The Rayne Institute, University College London, 5 University Street, London WC1E 6JJ, United Kingdom

[2]Cancer Research Technology, Wolfson Institute of Biomedical Research, Gower Street, London

Running title: Novel protein kinase D inhibitor characterisation

[^]Address correspondence to Ian C. Zachary or Ian M. Evans, BHF Laboratories, Department of Medicine, The Rayne Institute, University College London, 5 University Street, London WC1E 6JJ, United Kingdom, Tel. +44 20-7679-6620; Fax, +44 20-7679-6212; E-mail: i.zachary@ucl.ac.uk, i.evans@ucl.ac.uk

SYNOPSIS

Vascular endothelial growth factor (VEGF) plays an essential role in angiogenesis during development and in disease largely mediated by signalling events initiated by binding of VEGF to its receptor, VEGFR2/KDR. Recent studies indicate that VEGF activates protein kinase D (PKD) in endothelial cells to regulate a variety of cellular functions, including signalling events, proliferation, migration and angiogenesis. To better understand the role of PKD in VEGF-mediated endothelial function, we characterized the effects of a novel pyrazine benzamide PKD inhibitor, CRT5, in HUVECs. The activity of PKD isoforms 1 and 2 were blocked by this inhibitor as indicated by reduced phosphorylation at serines 916 and 876, respectively, after VEGF stimulation. The VEGF-induced phosphorylation of three PKD substrates, histone deacetylase 5, CREB and heat shock protein 27 serine 82 (HSP27), was also inhibited by CRT5. In contrast, CRT6, an inactive analogue of CRT5, had no effect on PKD or HSP27 serine 82 phosphorylation. Furthermore, phosphorylation of HSP27 at serine 78, which occurs solely via the p38 MAP kinase pathway was also unaffected by CRT5. In vitro kinase assays show that CRT5 did not significantly inhibit several PKC isoforms expressed in endothelial cells. CRT5 also decreased VEGF-induced endothelial migration, proliferation and tubulogenesis, similar to effects seen when the cells were transfected with PKD siRNA. CRT5, a novel specific PKD inhibitor, will greatly facilitate the study of the role of PKD signalling mechanisms in angiogenesis.

Keywords: endothelium, protein kinase C, angiogenesis,

Abbreviations: CREB, cAMP response element binding protein; ERK1,2, extracellular signal-regulated kinases 1 and 2; HDAC5, histone deacetylase 5; HUVEC, human umbilical vein endothelial cells; p38 kinase, p38 mitogen-activated protein kinase; PKC, protein kinase C; PKD, protein kinase D/PKCm; VEGF, vascular endothelial growth factor.

1. INTRODUCTION

Protein kinase Ds (PKD) are diacylglycerol (DAG)-stimulated serine/threonine protein kinases, originally classified as a sub-group of the protein kinase C family [1,2] but subsequently recognised to be a distinct subgroup of the calcium/calmodulin-dependent protein kinase family [3], only sharing significant homology to PKCs in the DAG-binding domain.

There are currently three known PKD isoforms, PKDs1-3. All three isoforms share the same basic structure consisting of a variable N-terminal regulatory domain and a C-terminal kinase domain, the latter with over 90% homology between the isoforms [4]. PKD2 differs from PKD1 in having a serine-rich linker between the two N-terminal zinc finger domains present in all three isoforms, whereas PKD3 lacks the alanine and proline-rich hydrophobic domain found at the N-terminus of PKDs1 and 2.

Activation of PKD can occur by multiple pathways, the primary one being non-classical PKC-dependent activation [5,6] resulting from phosphorylation at serines within the catalytic domain (ser744/748 in mouse PKD1, equivalent to serines 738/742 in human PKD1) [7], which occurs at the cell membrane following recruitment of both PKD and PKC by DAG. On PKD1 and 2, but not 3, there is also an autophosphorylation site near the C-terminus (ser916/876 in PKD1 and 2 respectively), which determines PKD tertiary structure and appears to be important for its interaction with other proteins, including 14-3-3 and PDZ proteins. PKD is predominantly localised in the cytosol, but can be translocated to the nucleus [8] or Golgi [4] after activation at the plasma membrane. The substrate consensus sequence for PKD-mediated phosphorylation is LXR(Q/K/E/M)(M/L/K/E/Q/A)S*XXXX, including a strong preference for leucine at the –5 position, and several target proteins have recently been identified including HSP27 and histone deacetylases 5 and 7 [9-12].

PKD has been implicated as a mediator in diverse cellular functions, including proliferation, survival, cellular trafficking and regulation of transcription. In endothelial cells PKD is activated by vascular endothelial growth factor (VEGF or VEGF-A), an essential angiogenic factor during development and in the pathogenesis of human pathologies including cancer and eye diseases [13,14]. There is growing evidence that endothelial cellular responses to VEGF are mediated at least in part through PKD [15]. We previously showed

that PKD is required for VEGF mediated endothelial migration and tube formation [10] and other studies have demonstrated the role of PKD in VEGF-induced phosphorylation of histone deacetylases, proliferation and migration [11,12]. Given the importance of PKD in VEGF-mediated angiogenesis, a pharmacological inhibitor would be a valuable biological tool for further investigation of PKD-mediated signalling but could also give rise to novel anti-angiogenic therapeutics. A recent study described effects of a specific PKD inhibitor in cancer cells [16], though subsequent work indicates that this compound is probably not specific for PKD [17]. Here we report the characterisation of a novel specific PKD inhibitor, CRT5, and investigate its effects on angiogenic processes in endothelial cells.

2. MATERIALS AND METHODS

2.1. Materials.

VEGF-A_{165} was from R & D Systems Ltd. (Abingdon, UK). SB203580 and GF109203X were from Calbiochem Inc (Nottingham, UK). Antibodies to total ERKs 1 and 2, total PKD, phospho-PKD (serines 744/748), phospho-PKD1 (serine 916), total CREB, phospho-CREB (serine 133), total HSP27 and phospho-HSP27 (serine 82) were from Cell Signalling Technology Inc (Herts, UK). The antibody to phospho-HSP27 (serine 78) was from Upstate Biotechnology Inc (Hampshire UK) and the antibody to phospho-PKD2 (serine 876) was from Universal Biologicals Ltd (Cambridge, UK). The antibody to total and phospho-HDAC5 (serine 498) were obtained from Insight Biotechnology Ltd (Wembley UK) and Autogen Bioclear (Wilts, UK) respectively. CRT5 was synthesised in-house at Cancer Research Technology [18]. CRT6 is a CRT5 analogue with the same core chemical structure indicated in reference 18. All other reagents were of the highest grade available.

2.2. Cell culture.

Human Umbilical Vein Endothelial Cells (HUVECs) were obtained from TCS CellWorks (Buckingham, UK) and cultured on gelatin-coated plates in endothelial basal medium (EBM; Cambrex BioScience Ltd, Nottingham, UK) supplemented with gentamycin-ampicillin, epidermal growth factor and bovine brain extract (Singlequots; Cambrex) and 10% (v/v) foetal bovine serum (FBS) (complete EBM). For experimental purposes, fully confluent HUVECs at passages 2-4 were pre-incubated overnight with 0.5% FBS in EBM prior to addition of factors and other treatments.

2.3 Compound screening, Kinase profiling and IC_{50} determination

Initially, inhibitors of PKD were identified by screening compounds for their ability to inhibit PKD1 in an in vitro kinase assay using purified recombinant His-tagged PKD1 kinase domain expressed in baculovirus (provided by Harold Jefferies, CRUK) and an IMAP detection system (Immobilized metal ion affinity-based fluorescence polarization; MDS Analytical Technologies Ltd, Berks UK). Compound libraries were obtained from the following companies: Maybridge, AsInEx, Bionet Research, Chembridge, Interbioscreen, and Specs.

Briefly, 12 nM recombinant PKD1 kinase domain (in 20% v/v glycerol) was mixed with 200 nM substrate (recombinant MAKAPK2, from MDS Analytical Technologies Ltd) and compound for screening (1.2 µM in DMSO; final DMSO concentration 4%) in assay buffer (25 mM Hepes pH 7.5, 2 mM $MgCl_2$). ATP was then added (10 µM final concentration) in a total assay volume of 30 µl. The assay mixture was incubated for 1 h at room temperature followed by the addition of 20 µl IMAP binding solution (MDS Analytical Technologies Ltd) and a further 2 h room temperature incubation in the dark. The fluorescence was then read on an Analyst HT plate reader (MDS Analytical Technologies Ltd).

Specificity of CRT5 was performed by in vitro kinase assays using a commercial kinase profiling service (Millipore UK Ltd, Herts, UK). The IC_{50}s for CRT5 inhibition of PKD1-3 were determined in vitro using IMAP. Briefly, 1 nM recombinant active PKD (in 20% v/v glycerol and assay buffer) was mixed with 200 nM recombinant MAKAPK2 and CRT5 (1.2 µM to 0.1 nM) in a total volume of 5 µl in assay buffer. After addition of 10 µM ATP (in assay buffer), the mixture wa incubated for 1 h at room temperature followed by the addition of 20 µl IMAP binding solution and a further 2 h room temperature incubation in the dark. The fluorescence was then read on an Analyst HT plate reader.

2.4. Cell viability Assay.

HUVECS were seeded in a 96-well plate at a density of 1.5 x 10^4 cells/well. Cells were incubated with the PKD inhibitor CRT5 (5 nM – 100 µM) in complete EBM. After 24 h 3-(4,5-dimethylthiaziazol-2-yl)2,5-diphenyl tetrazolium bromide (MTT; 0.5 mg/ml) was added to each well and incubated for a further 4 h. The medium was then removed and the cells were washed twice with PBS followed by the addition of 200 µl dimethyl sulfoxide (DMSO). After 15 min the resulting colour intensity was read at 570 and 650 nm.

2.5. Immunoblotting.

Cells were pre-treated with inhibitors in serum free medium for 30 min, followed by 10 min treatment with VEGF. After treatments, cells were washed with PBS and lysed in buffer containing 50 mM Tris-HCl pH 7.4, 150 mM NaCl, 1 mM disodium EDTA, 1% v/v Igepal CA-630, 0.5% w/v sodium deoxycholate, 0.1% w/v SDS, supplemented with phosphatase inhibitor cocktails SigmaPhos 1 and 2 and Complete™ protease inhibitor cocktail (Roche Diagnostics,

Welwyn Garden City, UK). Whole cell lysates were homogenised by brief sonication, adjusted to SDS-PAGE sample buffer (62.5 mM Tris HCl pH 6.8, 100 mM DTT, 2% w/v SDS, 10% v/v glycerol, 0.002% w/v bromophenol blue), and heated to 95˚C-100˚C for 3 minutes. Equivalent amounts of protein were separated by SDS-PAGE, and transferred to PVDF membranes (Millipore, Watford, UK). Membranes were blocked with 5% w/v non-fat dry milk and 0.1% v/v Tween-20 in PBS, for 1-2 h at room temperature, before being probed with the primary antibody by overnight incubation at 4°C. Detection was via a horseradish peroxidase-linked secondary antibody (Dako, Ely, UK) and ECL plus reagents (GE Healthcare), following the manufacturer's protocol. Autoradiograms of immunoblots were digitised on an ImageScanner (Amersham) and individual protein bands quantified with ImageJ software (US National Institutes of Health; http://rsb.info.nih.gov/nih-image/Default.html). Any differences in protein phosphorylation due to variations in loading were routinely corrected by normalizing to levels of the appropriate total protein.

2.6. Cell migration.

Transwell cell culture inserts made of transparent, low pore density polyethylene terephthalate (PET) with 8 μm pore size (Falcon; BD Biosciences, Oxford, UK), were inserted into a 24-well plate. Serum free media supplemented with or without 25 ng/ml VEGF-A_{165} or vehicle was placed in the bottom chamber and HUVECs in suspension (1.5 x 10^5 cell/well in serum free EBM) were added to the top chamber and incubated at 37˚C in for 4 h. HUVECs that had not migrated or had only adhered to the upper side of the membrane were removed before membranes were fixed and stained with a Reastain Quik-Diff kit (IBG Immucor Ltd, West Sussex, UK) using the manufacturer's protocol and mounted on glass slides. HUVECs that had migrated to the lower side of the membrane were counted in four random fields per well at 20 x magnification using an eye piece indexed graticule.

2.7. Proliferation.

Cell proliferation was assessed by direct counting as detailed in Liu et al [19]. Briefly, 3.2 x 10^4 cells per ml were allowed to attach to gelatin coated 24 well plate for 4 h. The complete medium was then replaced with 0.5% FCS/EBM with 2.5 μM CRT5 or vehicle. After 30 min, cells were treated with VEGF (25 ng/ml) or vehicle. After 48 h, cells were trypsinised and

counted using a Sysmex CDA-500 cell counter.

2.8. Tubulogenesis.

12-well plates were coated (750 µl per well) with PureCol Collagen (Nutacon BV, Leimuiden, Netherlands) solution (80% v/v in 0.01 M NaOH and M199 medium), which was allowed to solidify at 37˚C. HUVECs, transiently transfected with siRNAs as indicated, were then suspended in EBM containing 0.3% FCS, and overlaid onto the gel (1 x 10^5 cells/well) in the presence or absence of VEGF (25 ng/ml) and incubated for 16 hours at 37˚C. Digital photographs of cells were collected using the OpenLab Improvision system. Representative fields were selected and photos were taken of each well at x10 magnification. The area of linear tubule formation was calculated using Image J software. Areas of tubule formation were averaged between 4 fields and expressed as percentages of control untreated cells.

2.9. Transfection with PKD small interfering RNA (siRNA).

Specific siRNAs targeting PKD1 and PKD2 (Ambion Ltd Huntingdon, UK) were resuspended in nuclease-free water to yield a stock concentration of 50 µM. HUVECs in 6-well plates were allowed to reach ~70% confluence before transfection. Both PKD1 and PKD2 siRNAs were diluted to 1 µM each and combined with Opti-MEM media (Invitrogen, Paisley, UK), containing no serum or antibiotics, and incubated for 25 minutes with 10 µl Oligofectamine™ Reagent (Invitrogen) in a total volume of 200 µl. Thereafter, HUVEC monolayers were washed with Opti-MEM media and the complexes were added onto the cells at a final siRNA concentration of 200 nM each. In parallel wells, Silencer™ control siRNA (Ambion), which is a non-targeting scrambled siRNA, was used at 400 nM. After transfection for 4 hours, the medium was adjusted to 10 % FBS (v/v) and cells were incubated overnight. Media was then replaced with complete EBM and the cells incubated for a further 24 hours. The knockdown of PKD1 and 2 were then confirmed by immunoblotting.

2.10. Statistical methods.

Statistical analysis of differences in phosphorylation and migration was performed using one- or two-way analysis of variance (ANOVA) with *post hoc* analysis by Bonferroni's post test

where appropriate. Results are shown as means ± SEM, and $P<0.05$ was considered significant. Where necessary, data was logarithmically transformed prior to analysis to satisfy the criteria for ANOVA Non-linear regression analysis was performed using GraphPad Prism (San Diego, CA, USA).

3. RESULTS

3.1 Toxicity, Sensitivity and Specificity of the Protein Kinase D inhibitor

Initial screening of a diverse library containing approximately 55,000 compounds in an in vitro assay of PKD1 kinase activity identified several compounds which inhibited activity of PKD1. Of interest were pyridine benzamides and pyrazine benzamides, all with the core structure depicted in Fig. 1A [18], including the compound CRT5 (structure shown in Fig. 1A). The cytotoxicity of CRT5 was determined in HUVECs using an MTT assay. These data showed that CRT5 had an LD_{50} of 17 μM as established by non-linear regression analysis (Fig 1B) very similar to the cytotoxicity of this compound in cancer cell lines (data not shown). The biochemical IC_{50} of CRT5 as determined by inhibition of peptide substrate phosphorylation, was similar for all three PKD isoforms at 1, 2 and 1.5 nM for PKD1, 2 and 3 respectively. The specificity of CRT5 for PKD was also initially determined in an *in vitro* kinase assay, which included PKCs α, δ and ε, the major PKC isoforms expressed in HUVECs [20]. At 1μM, CRT5 completely inhibited PKDs1 and 2 as expected, but had little inhibitory effect on any of the PKC isoforms tested (Table 1). In addition, in a multi-kinase screen, CRT5 at 1 μM had little effect (<15% inhibition) on activity of other serine/threonine and tyrosine protein kinases, including Aurora-A, Calmodulin-activated kinase 1, Cdk-2, c-Raf, cSrc, Epidermal growth factor receptor, Glycogen synthase kinase 3β, IKKα, JAK-2, MAPKAPK2, MEK-1, PAK-2, Platelet-derived growth factor receptor-β, Akt/PKBα, ROCK-2, and RSK-1. Treatment of HUVECs with 5 μM CRT5 inhibited VEGF-induced phosphorylation of PKD1 at ser916 and PKD2 at the corresponding site, ser876 (Fig 1C). In contrast, PKD phosphorylation at ser744/748 was completely unaffected by CRT5 treatment, whereas the non-selective PKC inhibitor, GF109203X completely inhibited phosphorylation at these sites but caused little decrease in phosphorylation at ser916/ser876. The differential effects of CRT5 and GF109203X on PKD phosphorylation are readily explained by the lack of effect of CRT5 on PKC-dependent PKD phosphorylation, and CRT5 inhibition of subsequent PKD activity, demonstrated by the reduction of PKD autophosphorylation at ser916/ser876.

3.2 CRT5 inhibits PKD substrate phosphorylation

To further investigate the effects of CRT5 on PKD activity in the response of endothelial cells to VEGF, we tested its ability to inhibit the phosphorylation of proteins previously identified as PKD substrates: HSP27 (ser82), HDAC5 and CREB. In endothelial cells two of these substrates, HSP27 and CREB, are also phosphorylated via the p38 kinase pathway after VEGF activation [10,21]. Therefore, to distinguish between the role of PKD and p38 kinase pathways, we tested CRT5 in the presence or absence of the p38 kinase inhibitor, SB203580.

VEGF increased HSP27 phosphorylation at ser82 approximately 4-fold. CRT5 alone, significantly reduced VEGF-induced ser82 HSP27 phosphorylation, similar to the effect seen with the PKC inhibitor GF109203X alone (Fig 2A). Importantly, CRT5 in combination with SB203580, completely blocked HSP27 Ser82 phosphorylation, whereas SB203580 and CRT5 alone caused only partial inhibition (Fig. 2A). The effect of CRT5 is therefore strikingly similar to the effect of GF109203X, which in combination with SB203580 also completely abrogated HSP27 Ser82 phosphorylation (Fig. 2A), and also similar to the inhibitory effects of PKD knockdown using targeted siRNA previously reported by us [10]. Unlike ser82, HSP27 ser78 is not phosphorylated via PKD but is activated through the p38 kinase pathway [10]. Consistent with PKD-independent VEGF-induced ser78 phosphorylation, CRT5 or GF109203X had no effect on ser78 phosphorylation whereas SB203580 alone completely inhibited it (Fig 2B). In addition, CRT6, an analogue of CRT5 with the same core structure, that causes no inhibition of PKD at equivalent concentrations in vitro (results not shown), had no effect on either PKD ser916 or HSP27 ser82 phosphorylation at 5 μM (Fig. 2C).

The effect of CRT5 on CREB phosphorylation was similar to that seen with HSP27 ser82 phosphorylation. CRT5 alone partially reduced VEGF-induced CREB phosphorylation and GF109203X similarly significantly but partially inhibited this response, whereas SB203580 caused no significant decrease in CREB phosphorylation. However, CRT5 in combination with SB203580 caused a more marked inhibition of VEGF-induced CREB phosphorylation, and GF109203X with SB203580 also more strongly inhibited this response (Fig3A).

VEGF-induced HDAC5 phosphorylation was strongly inhibited by CRT5 at 5 μM, but in contrast to HSP27 and CREB phosphorylation, the combination of CRT5 and

SB203580 had no additional inhibitory effect. SB203580 alone had no inhibitory effect, confirming that HDAC5 is not activated via the p38 kinase pathway. Interestingly, GF109203X, either alone or in combination with SB203580, also had no significant inhibitory effect on VEGF-induced HDAC5 phosphorylation (Fig 3B), in contrast to previous reports [11]. Similar to effects of CRT5, in parallel cell cultures and treatments, knockdown of PKD1 and PKD2 in HUVECs using siRNA also significantly inhibited VEGF-induced CREB and HDAC5 phosphorylation (Fig. 4).

3.3 Protein kinase D inhibition inhibits VEGF-induced migration, proliferation and in vitro angiogenesis

VEGF induced a 5.8-fold increase in directed cell migration compared with vehicle (Fig. 5A) and pretreatment of HUVECs with CRT5 resulted in a significant reduction (by 42-51%) in the migratory response towards VEGF (Fig 5A). In contrast, the inactive CRT5 analogue, CRT6, had no significant effect on HUVEC migration. We also verified that, similar to our previous results, knockdown of PKD1 and PKD significantly reduced VEGF-stimulated endothelial cell migration with a similar effect to that of CRT5 tested in parallel cell cultures and treatments (Fig. 5B). VEGF treatment of HUVECs resulted in a 1.5-fold increase in cell proliferation over 48 h, compared with controls (Fig 5C), and this increase was completely inhibited by preincubation with CRT5 at 2.5 μM. CRT5 caused some decrease in the proliferation of control cells untreated with VEGF, but this effect was not statistically significant. VEGF induced a 2-fold increase in HUVEC tubule formation in a collagen-based assay (Fig 5D). CRT5 markedly inhibited VEGF-induced tubulogenesis, but had little effect on basal levels of tubulogenesis (Fig 5D), while CRT6 had no significant effect on tubule formation.

DISCUSSION

PKD has recently been implicated in many important cellular processes such as proliferation, migration and transcription. In particular, recent studies have indicated that PKD plays a major role in VEGF-mediated endothelial cell functions and in angiogenesis. Until recently, however, studies of the role of PKD have been hampered by the lack of specific inhibitors. While this work was in progress, effects of a PKD inhibitor, CID755673, were reported in a prostate cancer cell line [16]. CRT5 appears to be 100-fold more effective at PKD1 inhibition compared to CID755673 as determined by its IC_{50}. Furthermore, a recent study found that CID755673 enhances mitogenic signalling through a PKD-independent pathway and concluded that this compound cannot be regarded as a specific PKD inhibitor [17]. In contrast to CID755673, CRT5, the PKD-inhibitor used in this study, does not prevent PKD phosphorylation by PKC as shown by the lack of effect on VEGF-induced ser744/748 phosphorylation. CRT5 does, however, inhibit PKD kinase activity in vitro, and in intact endothelial cells, prevents the autophosphorylation of PKD1 and PKD 2 at ser916 and ser876, respectively. This is in marked contrast to the effects of the widely used PKC inhibitor, GF109203X, which strongly inhibited ser744/748 phosphorylation but had little effect on PKD autophosphorylation. The concentrations at which CRT5 inhibited PKD in intact endothelial cells are higher than those that inhibit PKD in cell-free assays using recombinant PKD. Such a difference is not unusual for pharmacological agents targeting intracellular enzymes and most likely reflects the cellular metabolism of CRT5 and/or its ability to penetrate the cell membrane. The differential effects of CRT5 and GF109203X together with *in vitro* kinase assay data, support the conclusion that the effect of CRT5 is highly unlikely to be due to inhibition of PKC activity. The specificity of CRT5 was further demonstrated by the observation that, while it partially inhibited HSP27 ser82 phosphorylation, it did not inhibit VEGF-stimulated HSP27 ser78 phosphorylation, which is mediated via the p38 kinase pathway in a PKD-independent manner. We have not investigated whether CRT5 also inhibits PKD3, but results from our previous study indicated that this isoform was not involved in either VEGF-induced HSP27 phosphorylation or migration [10].

It has recently been proposed that ser916 phosphorylation may not be an unambiguous marker of PKD activity [22]. It was therefore important to test whether CRT5 could block activation of known PKD substrates. HSP27 ser82 has a strong consensus PKD phosphorylation site and is an established downstream target of PKD in vitro and in cells [9,10]. Consistent with these data, CRT5 preincubation reduced HSP27 ser82 phosphorylation with an effect very similar to that seen with the non-selective PKC inhibitor, GF109203X, both in the presence and absence of the specific p38 kinase inhibitor, SB203580, suggesting that both CRT5 and GF109203X act on the same pathway. A notable feature of these findings is that while CRT5 and SB203580 acting alone caused only partial inhibition of HSP27 ser82 phosphorylation, the combination of these inhibitors completely blocked ser82 phosphorylation, consistent with the effects of GF109203X [10]. Furthermore, the effects of PKD inhibition on VEGF-induced HSP27 ser82 phosphorylation are in agreement with those seen when PKD expression is reduced by siRNA [10]. The VEGF-induced phosphorylation of two other recently identified PKD substrates, CREB and HDAC5, was also inhibited by CRT5. The conclusion that the inhibitory effects of CRT5 on VEGF-stimulated phosphorylation of HSP27 ser 82, CREB and HDAC5 are mediated via inhibition of PKD, is supported by the observation that targeted knockdown of PKDs 1 and 2 using siRNAs had a very similar inhibitory effect when compared directly with CRT5 in parallel cell cultures. Though we cannot preclude the possibility that PKD knockdown could have additional effects not caused by kinase inhibition, possibly mediated via kinase-independent protein-protein interactions, the effects of PKD siRNAs and CRT5 were in good agreement. The effects of CRT5 on CREB phosphorylation were broadly similar to those seen on HSP27 ser82, with greater inhibition occurring in the combined presence of CRT5 with SB203580. In contrast, HDAC5 phosphorylation was strongly inhibited by CRT5 alone, SB203580 having no additional effect. Surprisingly, GF109203X also had no effect on HDAC5 phosphorylation, in contrast to previously published data [11]. The reason for this discrepancy is unclear, but it may be explained by differences in HDAC5 regulation between bovine aortic endothelial cells as used by Ha et al [11] and HUVECs used in the present study. In addition, it may signify that VEGF can additionally activate PKD via a PKC-independent pathway in these cells. For example, it has been reported that PKD can

be activated by phosphorylation at tyrosine463 mediated by the Src pathway and independent of PKC [23]. This may also explain why GF109203X appears to be less effective than CRT5 at inhibiting PKD phosphorylation at ser916.

Since PKD is thought to play a pivotal role in VEGF-induced angiogenesis [10,11,15,24], we investigated whether CRT5 could disrupt the mechanisms associated with angiogenesis in endothelial cells. CRT5 markedly inhibited the migration and proliferation of HUVECs in response to VEGF stimulation, and reduced VEGF-induced in vitro angiogenesis in a collagen-based assay, while an inactive analogue of CRT5, CRT6, which does not inhibit PKD at similar concentrations, was unable to significantly disrupt migration or tube formation. The effects of CRT5 on migration and tubulogenesis are similar to those seen when PKD1 or PKD2 are knocked down with siRNA [10].

In conclusion we have shown that CRT5 acts as a specific inhibitor of PKD in the response of endothelial cells to VEGF, providing further support for the conclusion that PKD is an important mediator of VEGF receptor signalling and biological functions. This compound and/or its derivatives may have great potential, both as a biochemical tool and as a starting point for novel anti-angiogenic therapeutic drug development.

ACKNOWLEDGEMENTS

This work was supported by British Heart Foundation grant RG06/03/003 (I.Z.).

We dedicate this paper to the memory of Dr Lloyd Kelland now deceased.

REFERENCES

1. Valverde, A. M., Sinnett-Smith, J., Van Lint, J. and Rozengurt, E. (1994) Molecular cloning and characterization of protein kinase D: a target for diacylglycerol and phorbal esters with a distinctive catalytic domain. Proc. Natl. Acad. Sci. USA **91**, 8572-8576

2. Johannes, F. J., Prestle, J., Eis, S., Oberhagemann, P. and Pfizenmaier, K. (1994) PKCμ is a novel, atypical member of the protein kinase C family. J. Biol. Chem. **269**, 6140-6148

3. Manning, G., Whyte, D. B., Martinez, R., Hunter, T. and Sudar-Sanam, S. (2002) The protein kinase complement of the human genome. Science **298**, 1912-1934

4. Rykx, A., De Kimpe, L., Mikhalap, S., Vantus, T., Seufferlein, T., Vandenheede, J. R. and Van Lint, J. (2003) Protein kinase D: a family affair. FEBS Lett. **546**, 81-86

5. Zugaza, J. L., Sinnett-Smith, J., Van Lint, J. and Rozengurt, E. (1996) Protein kinase D (PKD) activation in intact cells through a protein kinase C-dependent signal transduction pathway. EMBO J **15**, 6220-6230

6. Zugaza, J. L., Waldron, R. T., Sinnett-Smith, J. and Rozengurt, E. (1997) Bombesin, vasopressin, endothelin, bradykinin, and platelet-derived growth factor rapidly activate protein kinase D through a protein kinase C-dependent signal transduction pathway. J. Biol. Chem **272**, 23952-23960

7. Iglesias, T., Waldron, R. T. and Rozengurt, E. (1998) Identification of in vivo phosphorylation sites required for protein kinase D activation. J. Biol. Chem **273**, 27662-27667

8. Rey, O., Sinnett-Smith, J., Zhukova, E. and Rozengurt, E. (2001) Rapid protein kinase D translocation in response to G protein-coupled receptor activation. Dependence on protein kinase C. J. Biol. Chem. **276**, 49228-49235

9. Doppler, H., Storz, P., Li, J., Comb, M. J. and Toker, A. (2005) A phosphorylation state-specific antibody recognizes Hsp27, a novel substrate of protein kinase D. J Biol Chem. **280**, 15013-15019

10. Evans, I. M., Britton, G. and Zachary, I. C. (2008) Vascular endothelial growth factor induces heat shock protein (HSP) 27 serine 82 phsophorylation and endothelial tubulogenesis via protein kinase D and independent of p38 kinase. Cell Signal. **20**,1375-1384

11. Ha, C. H., Wang, W., Jhun, B. S., Wong, C., Hausser, A., Pfizenmaier, K., McKinsey, T. A., Olsen, E. N. and Jin, Z-G. (2008) Protein kinase D-dependent phosphorylation and nuclear export of histone deacetylase 5 mediates vascular

endothelial growth factor-induced gene expression and angiogenesis. J Biol Chem. **283**,14590-14599

12. Wang, S., Li, X., Parra, M., Verdin, E., Bassel-Duby, R. and Olsen, E., N. (2008) Control of endothelial cell proliferation and migration by VEGF signaling to histone deacetylase 7. Proc. Natl. Acad. Sci. USA. **105**, 7738-7743

13. Ferrara, N., Gerber, H-P. and LeCouter, J. (2003) The biology of VEGF and its receptors. Nat. Med. **9**, 669-676.

14. Holmes DIR and Zachary I (2005) The Vascular Endothelial Growth Factor Family: Angiogenic Factors in Health and Disease. Genome Biol **6**, 209.1-209.10.

15. Qin, L., Zeng, H. and Zhao, D. (2006) Requirement of PKD tyrosine phosphorylation for VEGF-A^{165}-induced angiogenesis through its interaction and regulation of phospholipase Cγ phsophorylation. J Biol Chem. **281**, 32550-32558

16. Sharlow, E. R., Giridhar, K. V., LaValle, C. R., Chen, J., Leimgruber, S., Barrett, R., Bravo-Altamirano, K., Wipf, P., Lazo, J. S. and Wang, Q. J. (2008) Potent and selective disruption of protein kinase D functionality by a benzoxoloazepinolone. J Biol Chem **283** 33516-33526.

17. Torres-Marquez E, Sinnett-Smith J, Guha S, Kui R, Waldron RT, Rey O, Rozengurt E. (2010) CID755673 enhances mitogenic signaling by phorbol esters, bombesin and EGF through a protein kinase D-independent pathway. Biochem Biophys Res Commun. **391**, 63-68.

18. Raynham, T. M., Hammonds, T. R., Charles, M. D., Pave, G. A., Foxton, C. H., Blackaby, W. P., Stevens, A. P. and Ekwuru, C. T. (2008) Pyridine Benzamides And Pyrazine Benzamides Used As PKD Inhibitors. Patent number WO2008074997 26 June 2008

19. Liu, D., Evans, I., Britton, G. and Zachary, I. (2008) The zinc-finger transcription factor, early growth response 3, mediates VEGF-induced angiogenesis. Oncogene. **27**, 2989-2998

20. Gliki, G., Abu-Ghazaleh, R., Jezequel, S., Wheeler-Jones, C. and Zachary, I. (2001) Vascular endothelial growth factor-induced prostacyclin production is mediated by a protein kinase C (PKC)-dependent activation of extracellular signal-regulated protein kinases 1 and 2 involving PKC-δ and by mobilization of intracellular Ca^{2+}. Biochem. J. **353**, 503-512

21. Mayo, L. D., Kesseler, K. M., Pincheira, R., Warren, R. S. and Donner, D. B. (2001) Vascular endothelial cell growth factor activates CRE-binding protein by signaling through the KDR receptor tyrosine kinase. J. Biol. Chem. **276**, 25184-25189.

22. Rybin, V. O., Guo, J. and Steinberg, S. F. (2009) Protein kinase D1 autophosphorylation via distinct mechanisms at Ser^{744}/Ser^{748} and Ser^{916}. J. Biol. Chem. **284**, 2332-2343

23. Storz, P., Doppler, H., Johannes, F-J. and Toker, A. (2003) Tyrosine phosphorylation of protein kinase D in the pleckstrin homology domain leads to activation. J. Biol. Chem. **278**, 17969-17976

24. Avkiran, M., Rowland, A. J., Cuello, F. and Haworth, R. S. (2008) Protein kinase D in the cardiovascular system: emerging roles in health and disease. Circ. Res. **102**, 157-163

TABLE LEGEND

Table 1. Kinase specificity of CRT5. In vitro kinase assays showed that at 1 μM, CRT5 strongly inhibited protein kinase D while having little effect on a range of protein kinase C isoforms.

FIGURE LEGENDS

Figure 1. Structure, toxicity and specificity of CRT5. **A.** *Upper:* Core structure of PKD pyridine benzamide and pyrazine benzamide inhibitors, where R indicates one of several different functional groups, and X is either a nitrogen (N) or carbon covalently linked to a functional group (C-R). Further details of the structure of these compounds are provided in ref. 18. *Lower:* structure of CRT5. **B**. HUVECS were incubated with CRT5 (5 nM to 100 μM) for 24 h. Cell viability was estimated by MTT assay and plotted against log CRT5 concentration. Non-linear regression analysis was used to determine the LD50. **C.** Confluent HUVECs were pre-incubated for 30 min with either vehicle (Cont; 0.1% DMSO), 5 μM SB203580 (SB), 3 μM GF109203X (GF), 5 μM SB203580 plus 3 μM GF109203X (SB&GF) or 5 μM CRT5 with and without 5 μM SB203580 (CRT5&SB; CRT5, respectively) as indicated. This was followed by 10 min stimulation with vehicle (c) or VEGF (v; 25 ng/ml). Lysates were immunoblotted and probed with antibodies to PKD1 phosphorylated at ser916 or 744/748, PKD2 phosphorylated at ser876 and total PKD as indicated.

Figure 2. Effect of CRT5 on HSP27 phosphorylation. **A.** Confluent HUVECs were pre-incubated for 30 min with either vehicle (Cont; 0.1% DMSO), 5 μM SB203580 (SB), 3 μM GF109203X (GF), 5 μM SB203580 plus 3 μM GF109203X (SB&GF) or 5 μM CRT5 with and without 5 μM SB203580 (CRT5&SB; CRT5, respectively) as indicated. This was followed by 10 min stimulation with vehicle (c) or VEGF (v; 25 ng/ml). Lysates were immunoblotted and probed with antibodies to total and phosphorylated HSP27 (ser82). Data from 4 independent experiments were quantified by scanning densitometry and are presented as a ratio of HSP27 phosphorylation corrected for total HSP27 ± SEM

(arbitrary units). A representative blot corresponding to the quantified data is shown above the graph. Two-way ANOVA indicated significant treatment, inhibitor and treatment-inhibitor interaction effects ($P<0.005$). Significant differences of interest between treatments and inhibitors are indicated on the graph: *$P<0.05$, **$P<0.01$ and ***$P<0.001$ compared with VEGF alone by Bonferroni's post test. **B.** HUVECs treated as detailed in 2A were immunoblotted and probed with antibodies to phosphorylated HSP27 (ser78) and PKD2 (ser876). **C.** Confluent HUVECs were pre-incubated for 30 min with either vehicle (Cont), 5 μM SB203580 (SB), 3 μM GF109203X (GF), 5 μM SB203580 plus 3 μM GF109203X (SB&GF) or 5 μM CRT6 with and without 5 μM SB203580 (CRT6&SB; CRT6, respectively) followed by 10 min treatment with vehicle (c) or VEGF (v; 25 ng/ml. Lysates were immunoblotted and probed with antibodies to PKD phosphorylated at ser916, HSP27 (ser82) and total ERK as indicated.

Figure 3. Effect of CRT5 on CREB phosphorylation. A. Confluent HUVECs were pre-incubated for 30 min with either vehicle (Cont; 0.1% DMSO), 5 μM SB203580 (SB), 3 μM GF109203X (GF), 5 μM SB203580 plus 3 μM GF109203X (SB&GF) or 5 μM CRT5 with and without 5 μM SB203580 (CRT5&SB; CRT5, respectively) as indicated. This was followed by 10 min stimulation with vehicle (c) or VEGF (v; 25 ng/ml). Lysates were immunoblotted and probed with antibodies to total and phosphorylated CREB (ser133). Data from 3 independent experiments were quantified by scanning densitometry and are presented as a ratio of CREB phosphorylation corrected for total CREB ± SEM (arbitrary units). A representative blot corresponding to the quantified data is shown above the graph. Two-way ANOVA indicated significant treatment and inhibitor effects ($P<0.0001$ and $P<0.05$ respectively). Significant differences of interest between treatments and inhibitors are indicated on the graph: *$P<0.05$ compared with VEGF alone by Bonferroni's post test. **3B.** Effect of CRT5 on HDAC5 phosphorylation. Cells were treated as detailed for Fig 3A. Lysates were immunoblotted and probed with an antibody to phosphorylated HDAC5 (ser489). Data from 4 independent experiments were quantified by scanning densitometry and are presented as HDAC5 phosphorylation (arbitrary units) ± SEM. A representative blot corresponding to the quantified data is shown above the graph. Two-way ANOVA indicated a significant treatment effect

(P<0.0001). Significant differences of interest between treatments and inhibitors are indicated on the graph: *P<0.05 compared with VEGF alone by Bonferroni's post test.

Figure 4. Inhibition of PKD substrate phosphorylation by CRT5 and PKD knockdown. **A.** HUVECs were transfected with 200 nM siRNAs targeting PKD1 and PKD2, or 400 nM of a control siRNA (Scr). 48 h after transfection, and cells were then treated for a further 10 minutes with no addition (c), or with 25 ng/ml VEGF (v). In parallel cell cultures, confluent HUVECs were pre-incubated for 30 min with either vehicle (Cont; 0.1% DMSO), or 5 μM CRT5, followed by 10 min stimulation with vehicle or VEGF. Lysates were then immunoblotted with antibodies to total and phosphorylated HSP27 (ser82). Knockdown of PKD1 and 2 was confirmed using an antibody that recognises both PKD1 and PKD2 [10]. Data from at least 3 independent experiments were quantified by scanning densitometry and are presented as ratios of phosphorylated HSP27 to total HSP27 ± SEM (arbitrary units). A representative blot corresponding to the quantified data is shown above the graph. Two-way ANOVA indicated a significant interaction and treatment effects (P<0.05 and P<0.0001 respectively); *P<0.05 compared with VEGF+Scr siRNA or VEGF+vehicle by Bonferroni's post test. **B.** HUVECs treated as detailed in **A** were immunoblotted with antibodies to total or phosphorylated CREB. Two-way ANOVA indicated a significant interaction, inhibitor and treatment effects (P<0.005); *P<0.01 compared with VEGF control siRNA or VEGF vehicle respectively by Bonferroni's post test. **C.** HUVECs treated as detailed in **A** were immunoblotted with antibodies to total or phosphorylated HDAC5. Two-way ANOVA indicated a significant inhibitor and treatment effects (P<0.05 and P<0.001 respectively);*P<0.05 compared with Scr siRNA+VEGF or vehicle +VEGF by Bonferroni's post test.

Figure 5. Effect of CRT5 on VEGF-induced migration and tubulogenesis. **A**. HUVECs were trypsinised and incubated for 30 min in the presence of vehicle (Cont; 0.08% DMSO), 1 – 5 μM CRT5 or 5 μM CRT6 before being added to the upper chamber of a Transwell migration assay chamber. Vehicle (c) or VEGF (v; 25 ng/ml) was added to the lower chamber and the cells were allowed to migrate at 37˚C. After 4 h, the inserts were fixed, stained and migrated cells were counted. Quantified results expressed as the mean number of cells migrated per field from at least three independent experiments are shown.

Migration towards vehicle is represented by open bars and towards VEGF by closed bars. Data were analysed by one-way ANOVA; * p<0.05 compared to vehicle+VEGF.

B. HUVECs were transfected with 200 nM siRNAs to PKD1 and PKD2, or 400 nM control siRNA (Scr), for 48 h. In a parallel set of experiments, non-transfected HUVECs were trypsinised and incubated for 30 min in the presence of vehicle (Cont; 0.08% DMSO) or 5 μM CRT5. Cells were then used to determine migration in response to 25 ng/ml VEGF in a Transwell migration assay as described in Materials and Methods. Quantified results expressed as the mean number of cells migrated per field from at least three independent experiments are shown. Migration towards vehicle is represented by open bars and towards VEGF by closed bars. Two-way ANOVA indicated a significant inhibitor, interaction and treatment effects (P<0.0001). Significant differences of interest are indicated on the graph: *P<0.001 compared with Scr siRNA+VEGF or vehicle +VEGF respectively by Bonferroni's post test. **C.** HUVECs were seeded at a density of 3.2 x 10^4 cells per ml and allowed to attach to a gelatin coated 24 well plate for 4 h. The complete medium was then replaced with 0.5% FCS/EBM with 2.5 μM CRT5 or vehicle (Cont) or 10% FCS/EBM (hatched bar). After 30 min, cells were treated with VEGF (25 ng/ml, black bars) or vehicle (open bars) as indicated. After 48 h, cells were trypsinised and counted using a Sysmex CDA-500 cell counter. The results are expressed as the fold increase in cell number from the original seeding density from three independent experiments. Data were analysed by one-way ANOVA; * p<0.05 compared to vehicle+VEGF. **D.** HUVECs were trypsinised and incubated for 30 min in the presence of vehicle (Cont; 0.08% DMSO), 5 μM CRT5 or 5 μM CRT6 in EBM containing 0.3% v/v FCS. Cells were then plated onto a collagen base as described in Materials and Methods. Cells plated onto collagen were then incubated for 16 hours either with no addition (Control, open bars), or with 25 ng/ml VEGF (black bars). Tubulogenesis was quantitated with ImageJ. ANOVA indicates that CRT5 significantly reduced VEGF-mediated tube formation whereas CRT6 had no significant effect. *P < 0.05 compared with VEGF (no inhibitor) by Bonferroni's post test. Values (n ≥ 3) are means ± SEM, expressed as the area of tubules formed in pixels per field.

Biochemical Journal Immediate Publication. Published on 24 May 2010 as manuscript BJ20100578

Kinase	% inhibition (at 1μM CRT5)
PKCα	5
PKCβI	<1
PKCβII	<1
PKCγ	23
PKCδ	1
PKCε	<1
PKCη	<1
PKCι	10
PKCθ	2
PKCζ	<1
PKD1	98
PKD2	96

Table 1: Kinase specificity of CRT5

Biochemical Journal Immediate Publication. Published on 24 May 2010 as manuscript BJ20100578

Fig. 1

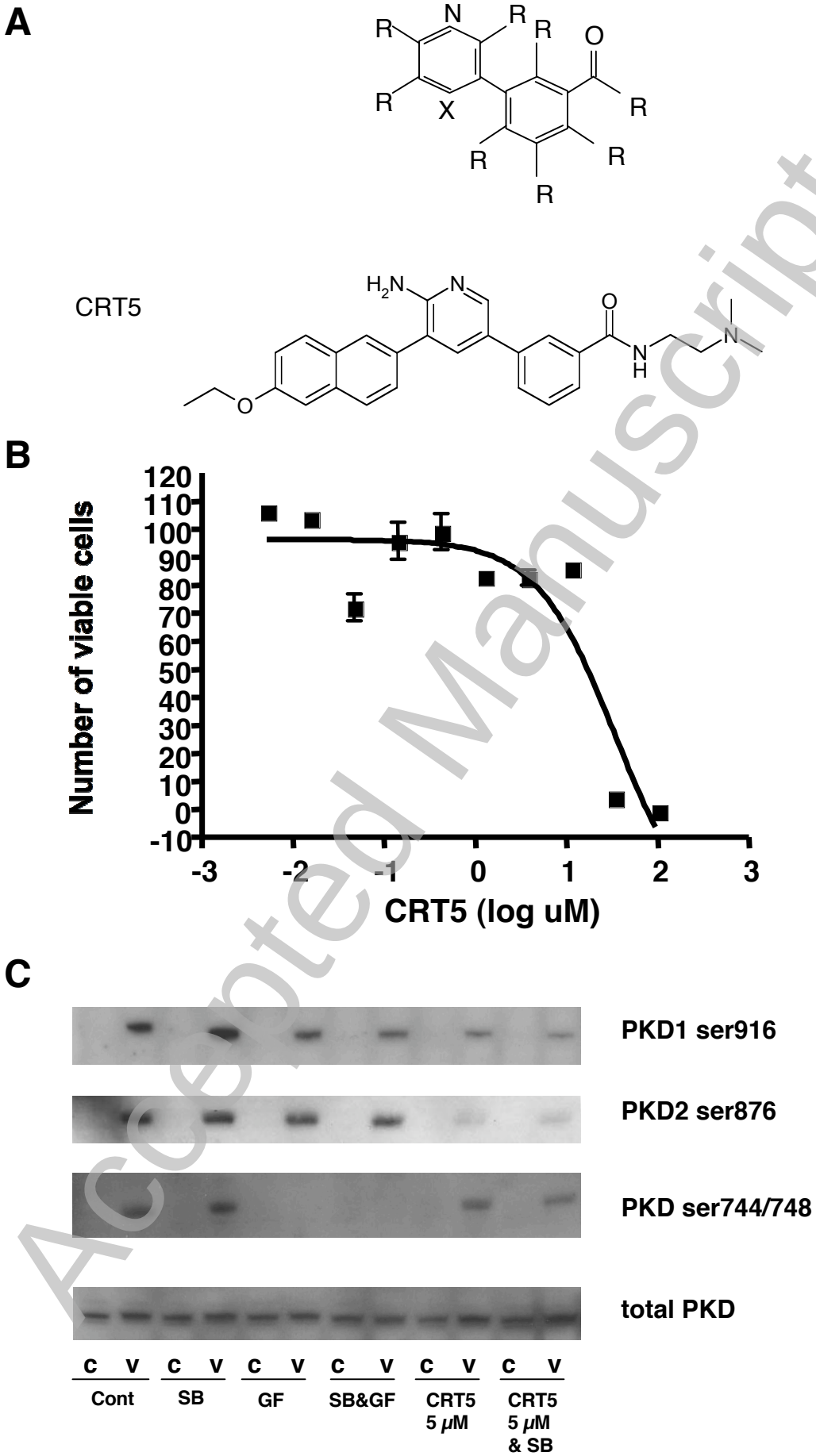

Biochemical Journal Immediate Publication. Published on 24 May 2010 as manuscript BJ20100578

Fig. 2

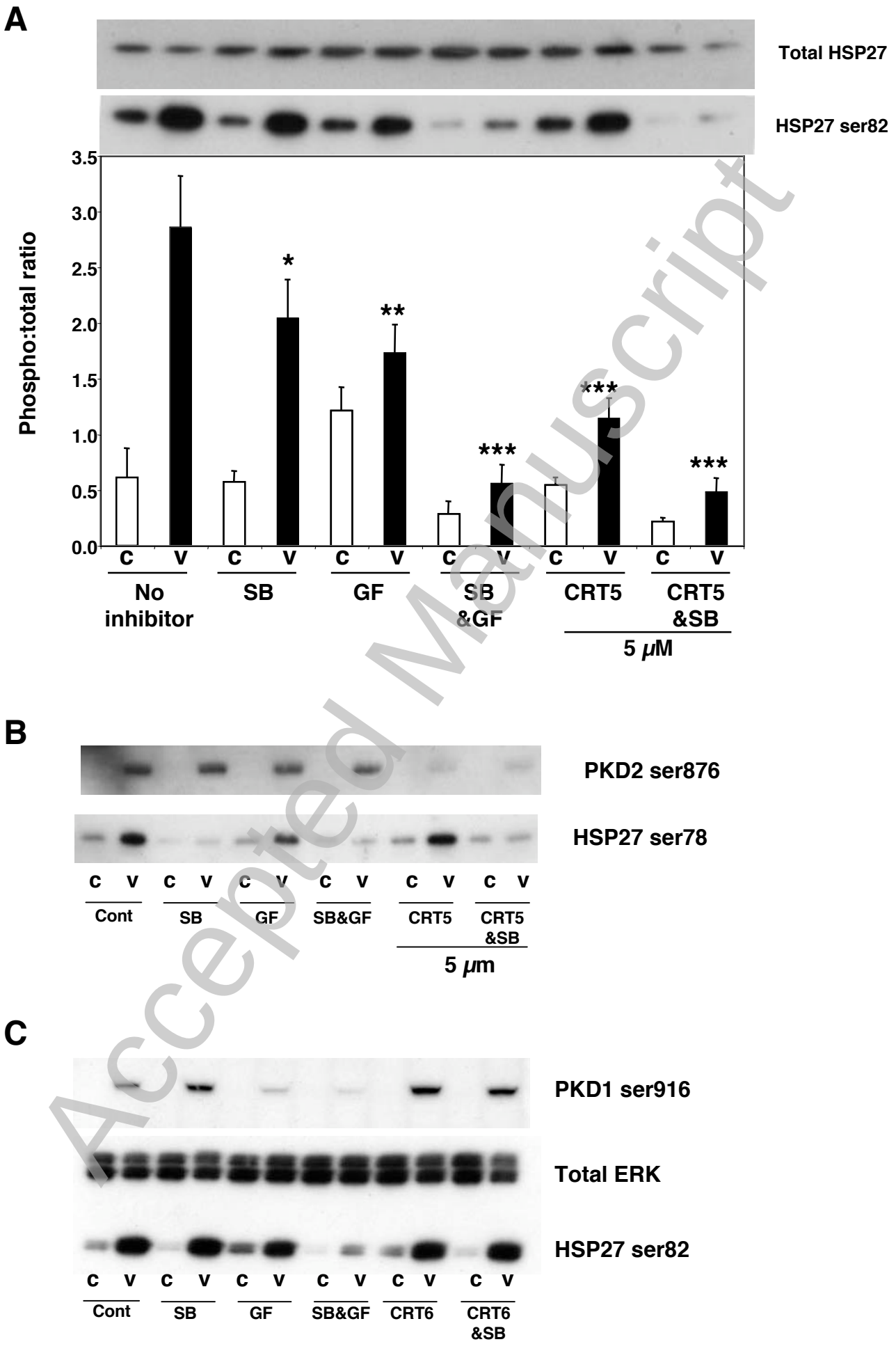

Biochemical Journal Immediate Publication. Published on 24 May 2010 as manuscript BJ20100578

Fig. 3

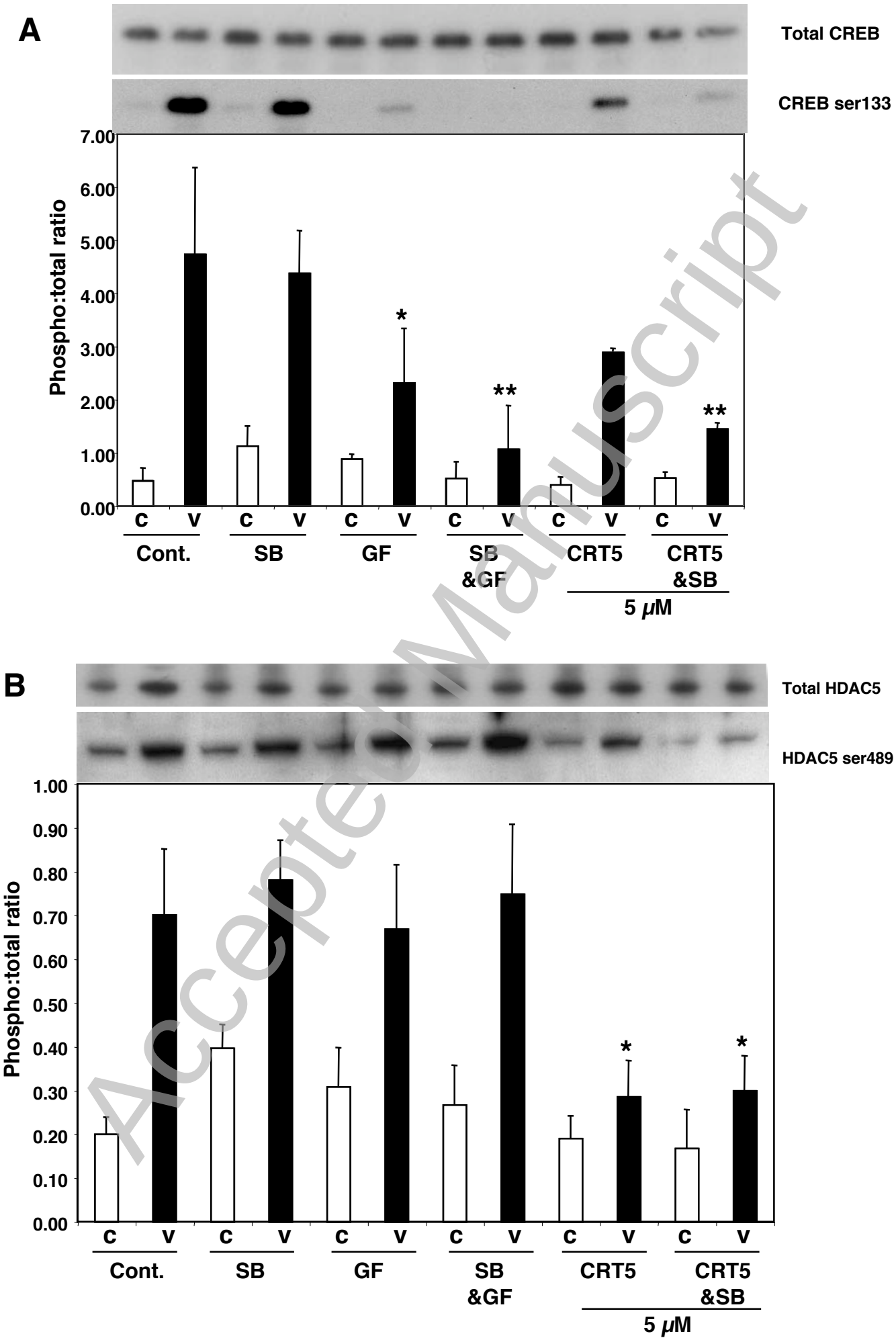

Biochemical Journal Immediate Publication. Published on 24 May 2010 as manuscript BJ20100578

Fig. 4

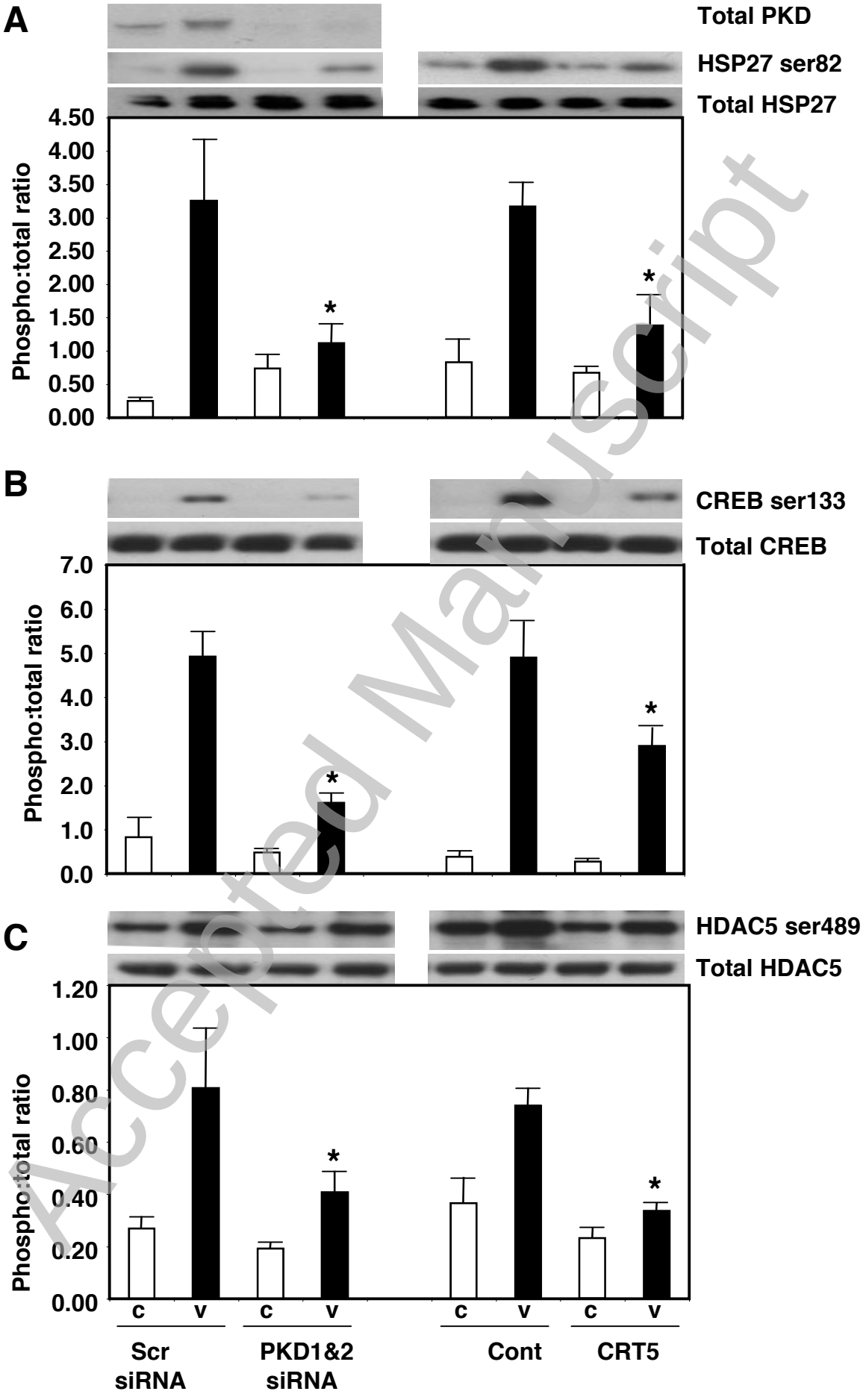

Biochemical Journal Immediate Publication. Published on 24 May 2010 as manuscript BJ20100578

Fig. 5

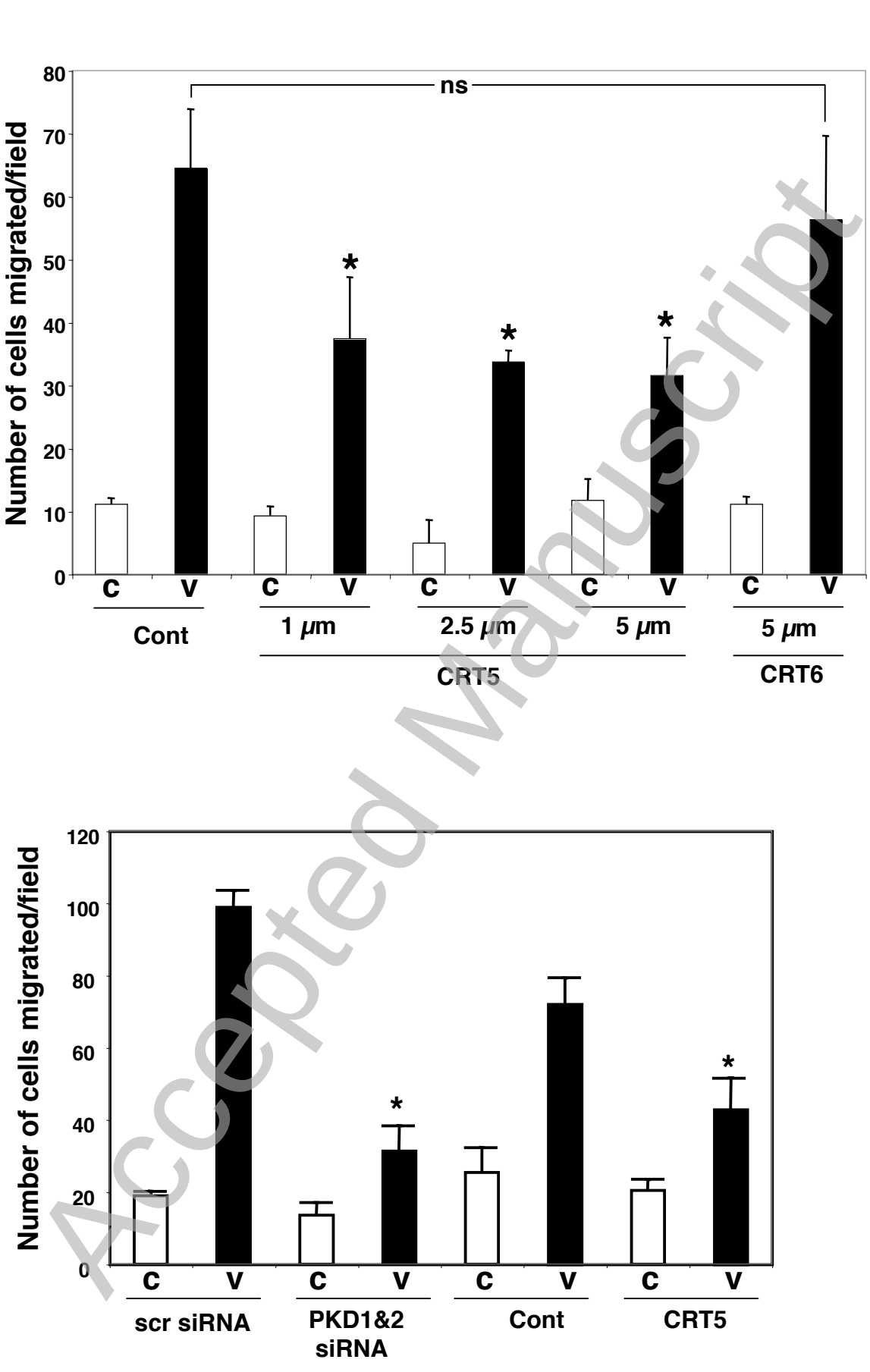

Biochemical Journal Immediate Publication. Published on 24 May 2010 as manuscript BJ20100578

Fig. 5